

# Impact of Dental Implant Surface Modifications on Adhesion and Proliferation of Primary Human Gingival Keratinocytes and Progenitor Cells



Chiara Giannasi, MS<sup>1</sup>  
 Giorgio Pagni, DDS<sup>2</sup>/Chiara Polenghi, DDS<sup>3</sup>  
 Stefania Niada, PhD<sup>1</sup>/Barbara Manfredi, PhD<sup>3</sup>  
 Anna Teresa Brini, PhD<sup>4\*</sup>/Giulio Rasperini, DDS<sup>5\*</sup>

The success of dental implants depends mainly on osseointegration and gingival sealing. Therefore, early attachment and spreading of epithelial cells might be critical for a positive outcome. Research in dental implant materials has primarily focused on surface roughness, defined by the average roughness (Ra) index, as it promotes the process of osseointegration. This study explored its influence on soft tissue attachment by looking mainly at adhesion, proliferation, and spreading of primary human cells belonging to the epithelial lineage. Characterized human gingival keratinocytes, gingival and epithelial progenitor cells were seeded on machined (S1; Ra = 0.3 to 0.6  $\mu\text{m}$ ), Ti-Unite (S2; Ra = 1.2  $\mu\text{m}$ ), and SLA (S3; Ra = 2  $\mu\text{m}$ ) implants. Cell adhesion with early proliferation and spreading were evaluated by combining a biochemical vitality test with imaging analyses. Findings showed that adhesion was significantly higher on S1 (36%  $\pm$  2%) and S2 (44%  $\pm$  7%) than on S3 (23%  $\pm$  6%), while early proliferation was slightly improved on S1. The resulting data, obtained through an innovative and easily reproducible *in vitro* method, suggest that implant surface roughness affects epithelial cell adhesion and proliferation. *Int J Periodontics Restorative Dent* 2018;38:127–135. doi: 10.11607/prd.3304

<sup>1</sup>Doctor, Department of Biomedical, Surgical and Dental Sciences, University of Milan, Milan, Italy; IRCCS Galeazzi Orthopaedic Institute, Milan, Italy.

<sup>2</sup>Doctor, Department of Biomedical, Surgical and Dental Sciences, University of Milan, Milan, Italy; Foundation IRCCS Ca' Granda Polyclinic, Milan, Italy.

<sup>3</sup>Doctor, Department of Biomedical, Surgical and Dental Sciences, University of Milan, Milan, Italy.

<sup>4</sup>Professor, Department of Biomedical, Surgical and Dental Sciences, University of Milan, Milan, Italy; IRCCS Galeazzi Orthopaedic Institute, Milan, Italy.

<sup>5</sup>Professor, Department of Biomedical, Surgical and Dental Sciences, University of Milan, Milan, Italy; Foundation IRCCS Ca' Granda Polyclinic, Milan, Italy.

\*Equal contribution

Correspondence to: Dr Anna Teresa Brini, Department of Biomedical, Surgical and Dental Sciences, University of Milan, Via Vanvitelli 32, 20129 Milan, Italy & IRCCS Galeazzi Orthopaedic Institute, Via Galeazzi 4, 20161 Milano, Italy. Fax: +39 02 50316987. Email: anna.brini@unimi.it

©2018 by Quintessence Publishing Co Inc.

Since the mid-1960s, dental implants have been successfully used to treat edentulous patients, with a survival rate higher than 90% after 15 years.<sup>1</sup> In the last decades, several physical and chemical treatments of the titanium surface have improved its biocompatibility in terms of biosafety and biofunctionality. Good clinical performance of an implant depends on osseointegration (ie, the formation of an effective interface between implant and bone) and gingival attachment, which occurs via the junctional epithelium (JE).<sup>2</sup> Several studies have primarily focused on bone response, leading to the development of surface optimization strategies to allow rapid osseointegration and to improve the strength and stability of bone-implant interaction.<sup>3</sup> It is widely accepted that rough surfaces, compared with machined ones, favor greater osteoblast anchorage, facilitating osseointegration.<sup>4</sup> However, as peri-implantitis represents a major cause of implant loss, recent research has focused on the interface between prosthesis and peri-implant soft tissues, stressing the importance of an adequate biologic seal.<sup>5</sup> This mucosal attachment consists of connective and epithelial components and protects the underlying tissues, such as alveolar bone, from bacteria and other pathogens. The epithelial attachment, being in direct contact

with the oral cavity, represents the first barrier and is essential for the innate immune response. Peri-implantitis occurs with little resistance from the host tissues once the mucosal seal fails and bacteria infect the cavity.<sup>6</sup> In periodontal disease the lesion never reaches the bone tissue, whereas in peri-implantitis the lesion invades the bone up to the marrow spaces, suggesting a weakness of the immune defense mechanism.<sup>7</sup> The pathogenesis of both periodontal and peri-implant disease clearly demonstrates that epithelial downgrowth is the first event characterizing attachment loss after bacterial accumulation.<sup>8,9</sup> At an advanced stage of the disease, the inflamed connective tissue in the apical part of the peri-implant lesion is in direct contact with the biofilm on the implant surface.<sup>9</sup> Recent clinical studies indicate that rough surfaces reduce the strength of soft tissue attachment and affect the efficacy of antimicrobial treatments.<sup>10,11</sup> Several groups are still unraveling the structural and functional biology of the implant-tissue interface.<sup>5,12,13</sup> Given the importance of mucosal interface for the long-term stability of titanium implants, the present authors evaluated the effect of three dental implants on human primary cells deriving from tissues involved in the onset of the epithelial sealing around the prosthesis. Through a rapid and sensitive *in vitro* analysis, the short-term impact of the implants' physical and topographic features on cell behavior was investigated. Gingival keratinocytes, gingival progenitor cells, and epithelial progenitor cells were isolated, characterized, and

maintained in culture on machined (S1), Ti-Unite (S2; Nobel Biocare), and SLA (S3, Straumann) dental implants. Cell adhesion, proliferation, spreading, and morphology on each were then analyzed with the aim to propose a link between the data and clinical success or failure.

## Materials and Methods

### *Cell Isolation and Expansion*

All cell populations were obtained from waste tissues of healthy donors undergoing oral or plastic surgery, following the procedure approved by IRCCS Galeazzi Orthopaedic Institute (PQ 7.5.125, version 4, 22.01.2015). Written informed consent was obtained from all patients. Gingival keratinocytes (hGKs) and progenitor cells (hGPCs) were collected from five donors, while epithelial progenitor cells (hEPCs) were collected from two donors.

### **Gingival Keratinocytes**

Specimens of gingival epithelium were digested with 0.1% Trypsin 0.04% ethylenediaminetetraacetic acid (EDTA) and centrifuged. Pellets were then resuspended in complete Roswell Park Memorial Institute (cRPMI) medium (RPMI1640 [Sigma Aldrich] supplemented with 5% fetal bovine serum [FBS] [HyClone, Thermo Scientific], 25 mM HEPES [Corning], 2 mM L-glutamine [Sigma Aldrich], 50 U/mL penicillin, and 50 µg/mL streptomycin [Sigma Aldrich]) and plated to favor primary cell outgrowth, as previously described.<sup>14,15</sup>

### **Gingival Progenitor Cells**

Gingival progenitor cells (hGPCs) were isolated from fragments deriving from reductive gingivoplasty, as previously described.<sup>16</sup> Briefly, samples were washed in phosphate-buffered saline (PBS), minced with surgical scissors, and digested with type I collagenase (50 U/mL, Life Technologies, 3:1 v/w ratio). After centrifugation, cells were cultured in complete Dulbecco's modified Eagle's medium (cDMEM) (DMEM [Sigma Aldrich] supplemented with 10% fetal bovine serum, 2 mM L-glutamine, 50 U/mL penicillin, and 50 µg/mL streptomycin).

### **Epithelial Progenitor Cells**

Skin obtained as waste material from abdominoplasty was quickly washed in 70% ethanol. The epithelial layer, isolated from loose connective tissue and subcutaneous fat with tweezers and a scalpel, was mechanically minced and digested with 0.1% Trypsin 0.04% EDTA. After centrifugation, cells were cultured in cDMEM.

All cell types were kept in a controlled environment (37°C in a humidified atmosphere with 5% CO<sub>2</sub>) and expanded. Keratinocytes and progenitor cells were used in the third and fourth passage, respectively.

### *Cell Characterization*

Cell morphology and proliferation rate were determined for all cell types. For hGPCs and hEPCs, additional features including clonogenicity, phenotypic profile, and multidifferentiative ability were also analyzed.

### Morphology

Cells were fixed and stained with Diff-Quik Kit (Medion Diagnostics).

### Cell Proliferation

A quantity of  $8 \times 10^3$  cells/cm<sup>2</sup> were cultured from second to fourth passage and detached when the cells were 80% to 90% confluent. Population doubling time (DT) was calculated as follows:

$$DT = \Delta t \times \ln 2 / \ln(N_c / N_p)$$

where  $\Delta t$  = hours between passages,  $N_c$  = number of collected cells, and  $N_p$  = number of plated cells.

### Cadherin Expression

The hGKs were seeded on 1-cm-diameter glass cover slips or on implants. After 3 days, cells were fixed in 4% paraformaldehyde, permeabilized with 0.1% Triton X-100 and incubated overnight at 4°C with a monoclonal antibody raised against pan Cadherin (clone CH-19, C1821, Sigma Aldrich). Specific binding was revealed with a polyclonal goat antimouse antibody conjugated to AlexaFluor 488 (ab150113, Abcam), and samples were analyzed by either wide-field fluorescence microscopy (Olympus BX51) or confocal microscopy (Leica TCS SP5 AOBS).

### Colony-Forming Unit–Fibroblast (CFU-F) assay

The hGPCs and hEPCs were serially diluted in six-well plates starting from 800 cells/well and cultured for 14 days in modified cDMEM (20% FBS). Then cells were fixed in methanol and stained with 2 mg/mL Crystal Violet (Fluka). Colonies with at least 25 cells were considered.

### Flow Cytometry Analysis

The hGPCs and hEPCs were analyzed by fluorescence-activated cell sorting (FACS), as previously described.<sup>17</sup> Briefly, cells were incubated for 30 minutes at 4°C with monoclonal antibodies raised against human CD73, CD90, CD105, or CD45, either FITC- or PE-conjugated. Samples were acquired by FACSCalibur flow cytometer (Becton Dickinson) and analyzed using CellQuestPro software (BD Bioscience).

### Osteogenic Differentiation

Cells were cultured up to 3 weeks in cDMEM (CTRL), or osteoinductive medium (OSTEO: cDMEM supplemented with 10 nM cholecalciferol, 10 nM dexamethasone, 10 mM glycerol-2-phosphate, and 150  $\mu$ M L-ascorbic acid-2-phosphate; all reagents Sigma Aldrich). Osteogenic differentiation was assessed through Sirius Red staining (Fast Red 80, Sigma Aldrich) to evaluate collagen production and Alizarin Red-S staining (Fluka) to depict mineral deposition, as previously described.<sup>18</sup>

### Adipogenic Differentiation

Cells were cultured in either CTRL or adipogenic medium (ADIPO: cDMEM supplemented with 500  $\mu$ M 3-isobutyl-1-methylxanthine [IBMX], 1  $\mu$ M dexamethasone, 200  $\mu$ M indomethacin, and 10  $\mu$ g/mL insulin; all reagents Sigma Aldrich) for 14 days. Samples were then fixed in 10% formalin and stained with Oil Red-O (BioOptica) to assess lipid vacuole formation.<sup>18</sup>

### Dental Implants

In this study, three commonly used surface topographies were considered: machined (S1 provided by iRES Group), Ti-Unite (S2, Nobel Biocare) and SLA (S3, sandblasted and acid etched, Straumann).<sup>19,20</sup> A machined surface is an untreated surface characterized by an anisotropic distribution that creates a Ra around 0.3 to 0.6  $\mu$ m. Ti-Unite is a highly crystalline biomaterial characterized by a thick layer of titanium oxide (up to 10  $\mu$ m) with a moderately rough porous surface (Ra = 1.2  $\mu$ m). SLA surface is a moderately rough surface (Ra = 2  $\mu$ m) obtained through a large grit sandblasting process that creates a macroroughness on the Ti surface, followed by strong acid etching that produces 2- to 4- $\mu$ m micropits.

Implants with variable shapes and sizes were longitudinally abraded in half to provide a flat surface that ensured good stability during the experiments. All the implants were cleaned and sterilized for clinical use.

### Cell Adhesion and Growth on Implants

#### Cell-Seeding Procedure

Implants were positioned inside the wells of a 24-well plate, previously coated with 1% agarose to prevent cell spreading on tissue-culture polystyrene. To achieve an efficient and uniform cell distribution, a small volume (10  $\mu$ l) of freshly mixed cell suspension at high ( $5 \times 10^4$  hGPCs/implant) or low density ( $10^4$  cells/implant for hGKs

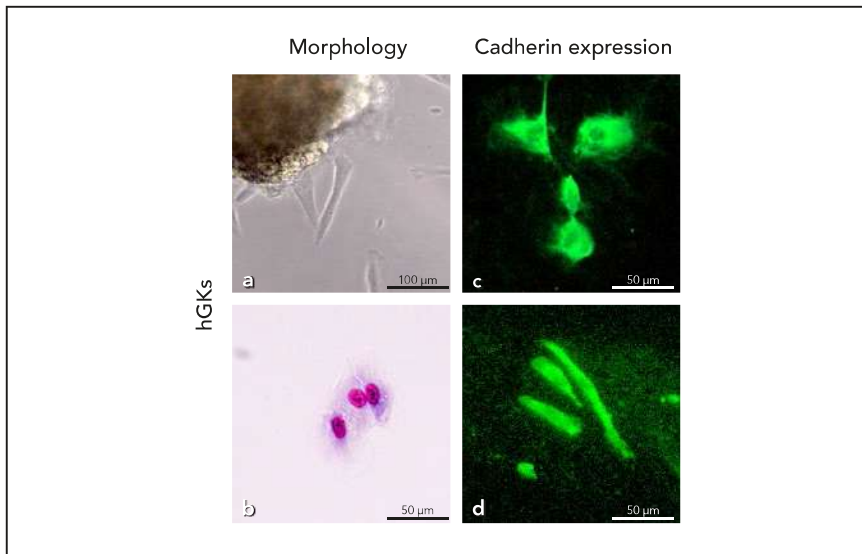


**Fig 1** Characterization of human gingival keratinocytes (hGK). (a) hGK outgrowth from a gingival specimen. (b) Morphology by Diff-Quik staining. (c) Immunostaining for Cadherin expression of hGKs on coverslip. (d) Immunostaining for Cadherin expression of hGKs on implant.

and hEPCs) was added to the surface of the implants. Culture medium was added after 90 minutes, a suitable time span to allow cell adhesion and prevent cell suspension dehydration. Simultaneously, to indirectly quantify the number of cells present on the implants over time, a standard curve for each cell type was set starting from  $8 \times 10^4$  cells/mL following serial dilutions with a ratio of 1:2.

#### Viability Assay

Samples were incubated in a culture medium supplemented with 10% AlamarBlue (Thermo Fisher Scientific) at 37°C in the dark. Four hours later, supernatants were transferred to black-bottom 96-well plates and fluorescence was read with a Wallac Victor II. Data were obtained at 24 hours for adhesion and after 3 days for proliferation by compar-

ing cells seeded on dental implants with their standards. Adhesion is expressed as percentage of viable cells on implants in respect to the number of seeded cells set as 100%. Cell proliferation is shown as percent of growth, considering the number of adherent cells at 24 hours as 100%.

#### Viable Cell Detection by Stereo- and Confocal Microscopy

Cells maintained on the implants for 4 days were incubated for 20 minutes with Calcein-AM, following LIVE/DEAD Cell Assay (Thermo Fisher Scientific). Images of the central area of each implant were acquired by fluorescent stereomicroscope (Leica M205FA) or confocal microscope (Leica TCS SP5 AOBs). Single images that allowed a three-dimensional reconstruction of cell distribution were obtained

by merging the Z stacks. To quantify the number of viable cells on the implants, images were analyzed by Fiji software (ImageJ).

#### Statistical Analysis

Unless otherwise stated, data are expressed as mean  $\pm$  SEM and statistical analysis was performed using one-way analysis of variance by GraphPad Prism 6. Differences were considered significant at  $P < .05$ .

## Results

### Characterization of Primary Cell Cultures

The hGKs displayed a typical squared shape and showed a strong expression of Cadherins when cultured in standard conditions and on implants, without major differences between the two settings (Fig 1). On the contrary, progenitor cells (hGPCs and hEPCs) exhibited the fibroblast-like morphology with elongated cytoplasmic processes peculiar of adult stem cells (Fig 2). The doubling time of  $75.3 \pm 18$  hours for hGKs was slower compared to hGPC ( $49.1 \pm 7$  hours) and hEPC ( $42.2 \pm 9$  hours) (Table 1). These last cell populations displayed a mean clonogenic ability of about 25% (Table 1). Both cell types expressed on their cell membrane the mesenchymal markers CD90 (> 97%), CD73 (> 93%), and CD105 (> 94%), while they lacked the peculiar hematopoietic marker CD45 (data not shown). Furthermore, osteogenic stimuli promoted

a mild upregulation of collagen production and calcified extracellular matrix deposition with respect to CTRL cells. After adipogenic induction, no morphologic change was observed in hGPCs and just a few lipid vacuoles were present in hEPC cytoplasm (Fig 2).

*Adhesion and Growth of Primary Human Cells on Titanium Implants*

As shown in Fig 3a, S2 implants showed the most pronounced cell adhesion regardless of the cell type. Indeed,  $44\% \pm 7\%$  of seeded cells attached to S2 surfaces. S3 implants displayed the least efficient performance, with a mean adhesion of  $22\% \pm 6\%$ . With  $36\% \pm 2\%$  cell adhesion, S1 appeared almost as good as S2. In addition, S1 slightly improved short-term proliferation (with an increase of  $200\% \pm 12\%$  in respect to day 1), whereas S2 ( $157\% \pm 11\%$ ) and S3 ( $152\% \pm 27\%$ ) demonstrated similar cell growth (Fig 3b). As a proof of concept, hGK growth was evaluated up to day 10 to determine implant long-term biocompatibility and the results on S2 showed that cell number increased over time, matching the classical exponential kinetic model of standard culture conditions (Fig 3c). These cell adhesion and growth trends on different surfaces were confirmed by fluorescence microscopy. The stereomicroscopy analysis indicated that the distribution of gingival progenitors on the two implants that showed the highest growth rate and cell attachment

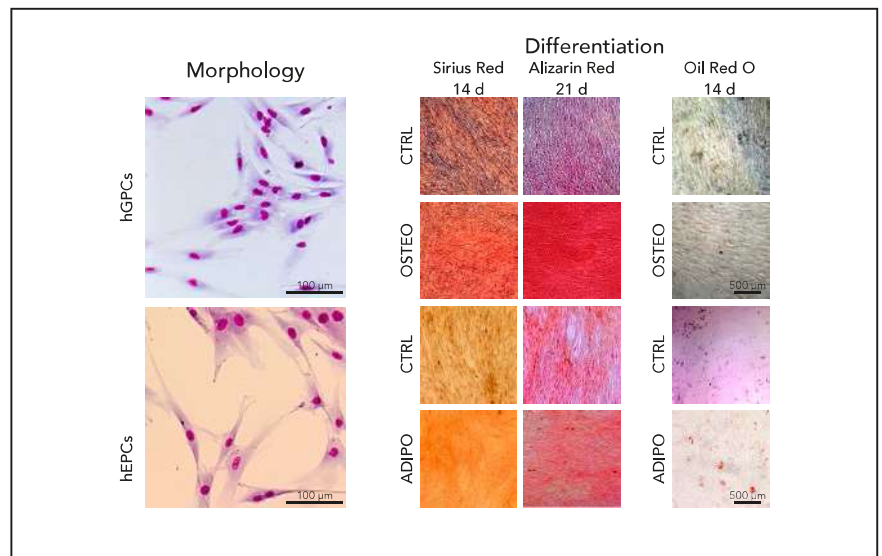


**Fig 2** Human gingival progenitor cell and epithelial progenitor cell features: morphology by DiffQuik staining and 14- or 21-day differentiation (left, middle, and right panels, respectively). In osteodifferentiated cells, collagen deposition was determined by Sirius Red staining while calcified extracellular matrix formation was determined by Alizarin Red staining. Adipo-induced cells were stained by Oil Red O.

**Table 1 Cell Proliferation Rate Expressed as Doubling Time (DT), Clonogenic Ability as Percentage of Number of Colonies/ Seeded Cells, and Differentiative Ability Expressed as Percentage of Increase with Respect to Undifferentiated Cells**

	DT (h)	CFU-F (%)	% increase with respect to CTRL		
			OSTEO		ADIPO
			Collagen deposition	Calcified ECM production	Liquid droplet formation
hGKs	75.3 ± 18	ND	ND	ND	ND
hGPCs	49.1 ± 7	19.9 ± 11	+82	+360	+10
hEPCs	42.2 ± 9	29.6 ± 9	+150	+82	+20

hGKs = gingival keratinocytes; hGPCs = gingival progenitor cells; hEPCs = epithelial progenitor cells; CFU-F = colony-forming unit—fibroblasts; ECM = extracellular matrix; ND = not determined.

(S1 and S2) was comparatively more homogenous in respect to S3 (Fig 3d). To provide a snapshot of the presence of cells on different areas of the implants at day 4, laser scan confocal microscopy analysis was performed. Cells were easily countable, and their morphology and

spreading were clearly discernible (Fig 4). Metabolically active cells were observed uniformly spread on S1, regardless of the cell type (hGKs or hEPCs), suggesting that the machined surface might favor cell growth (Fig 4b). This analysis also showed that epithelial cell

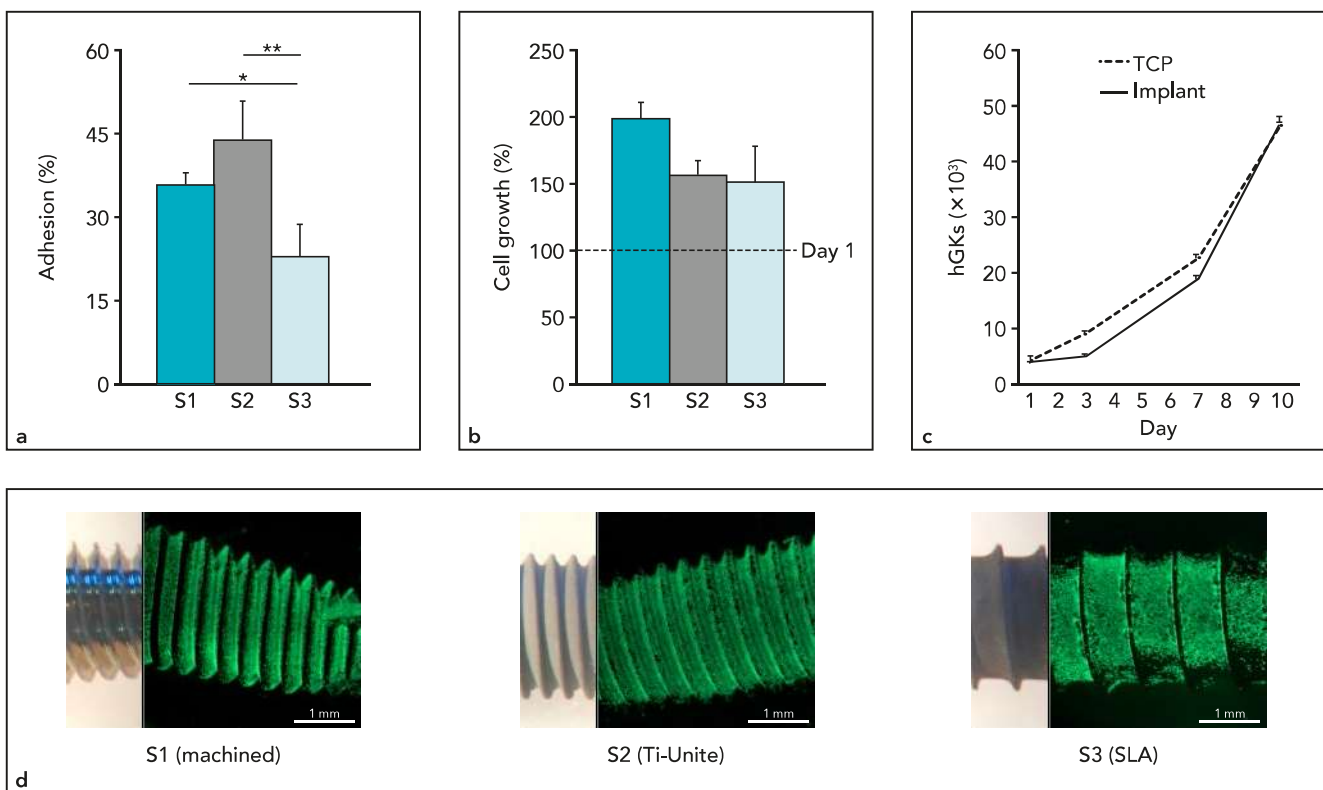


**Fig 3** Primary cell adhesion and proliferation on dental implants. (a) Comparison of cellular adhesion on different implants. Data, derived from three independent experiments, are expressed as percentage of viable adherent cells with respect to the seeded ones. \* $P < .05$ ; \*\* $P < .01$ . (b) Cellular proliferation on the implants 3 days after seeding. Data from three independent experiments are expressed as percentage of cell growth, with the number of adherent cells at day 1 on each implant set as 100%. (c) Human gingival keratinocyte proliferation on S2 compared to standard culture condition on tissue culture polystyrene (TCP) up to 10 days. Data are expressed as mean  $\pm$  SD of three technical replicates. (d) Stereomicroscopic images of empty implants (bright field) or loaded with human gingival progenitor cells and Calcein-stained on day 4.

attachment and the spreading observed on S3 implants were less pronounced, confirming the previous results regarding cell vitality (Fig 4b).

## Discussion

In the present study, it was investigated whether adhesion and short-term proliferation of human primary cells of epithelial lineage are influenced by implant surface charac-

teristics. Through a combined cell biology approach, the effects of surface roughness of three dental implants on cell attachment and short term growth were evaluated in vitro.

Purified and characterized isolated gingival and skin progenitor cells appear to belong to the adult stem cell type, according to the mesenchymal stem cell (MSC)-defining criteria.<sup>21</sup> Indeed, their clonogenic ability, together with their osteogenic potential, nicely align

with human bone marrow stromal cells and human adipose-derived stem cells.<sup>22</sup> However, these progenitor cells scarcely differentiate into adipocytes, and their low adipogenic potential might depend on the harvesting source, as previously demonstrated for MSCs of other origins.<sup>23</sup> Since terminally differentiated keratinocytes express a high level of Cadherins, a class of transmembrane proteins responsible for cell-to-cell adhesion, proliferation, migration, and maintenance of an

effective barrier function, a more pronounced expression of these proteins by gingival keratinocytes was observed compared to MSCs (data not shown).<sup>24</sup> The three-dimensional culture conditions did not affect this parameter. The authors believe that these three primary cell populations are effective tools for monitoring variations in adhesion and growth induced by the modified surfaces of dental implants. Cell attachment of progenitors and terminally differentiated cells was significantly reduced only on S3 in comparison to S2 and S1 surfaces, indicating that roughness of inert biomaterials is not the most important feature in favoring cell adhesion. Since the Ra index of S2 and S3 was quite similar, other factors could be involved in promoting or reducing initial cell adhesion. Mild improvement was seen in the proliferation rate of adherent cells on S1 that was further confirmed after observing cell spreading through stereo- and confocal microscopy.

A recent preclinical study by Atsuta et al<sup>25</sup> showed no difference between machined and rough implants on epithelial attachment at 4 weeks of follow-up. However, at 16 weeks, they described a weaker and thinner epithelial attachment around rough implants. Their *in vitro* data are consistent with the present observations and suggest that machined implants, compared to rougher surfaces, favor better cell migration with proliferation and expression of adhesion molecules. All these data correspond with the results found by Baharloo et al,<sup>10</sup> who demonstrated a reduced epithelial cell attachment

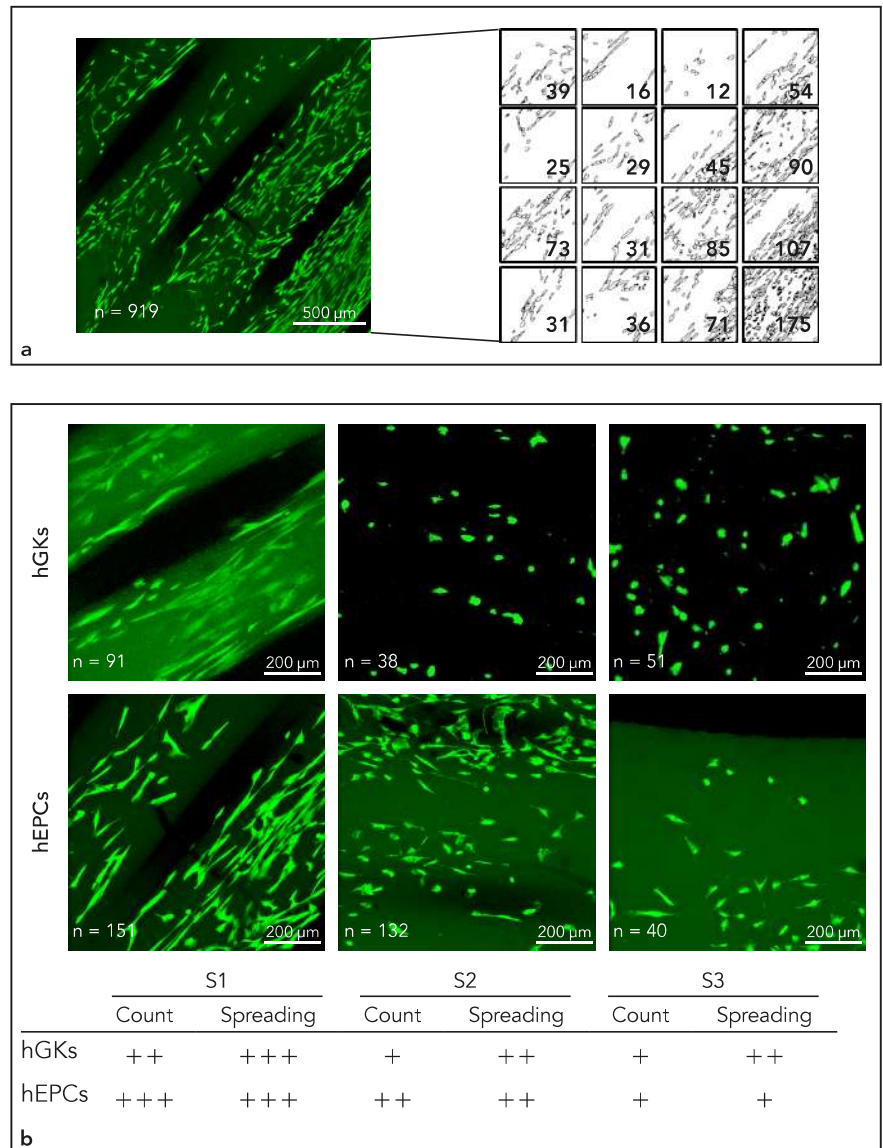


**Fig 4** Analysis of cell growth by confocal microscopy. (a) Representative image of Calcein-stained human epithelial progenitor cells (hEPCs) cultured on S1 for 4 days and its quantitative analysis using Fiji software. The number of counted cells for each selected area is indicated. (b) Confocal microscopy images of viable human gingival keratinocytes (hGKs) and hEPCs seeded on S1, S2, and S3 for 4 days and then stained with Calcein. n: cell count determined by Fiji software. At least three images were acquired for each magnification (×50 and ×100) and analyzed. The arbitrary scores +/++/+++ for cell growth and spreading indicate poor/good/optimal performance and were attributed by three independent blind operators on the basis of cell count and distribution through the implants (homogeneity, presence/absence of clusters, and maintenance of cell morphology), respectively.

and spreading on rough surfaces in comparison to machined. Several studies reviewed by Esposito

et al<sup>26</sup> on different types of dental implants provided evidence that turned implants reduce the risk of

peri-implantitis onset over a 3-year period compared to rough surfaces. More recently, Simion et al<sup>27</sup> showed good clinical performance of machined implants in sinus-lifted posterior maxilla, evaluating the survival rate over a 12-year period with regular follow-up. In this retrospective study, the rate of implant failure appeared low and the risk of peri-implantitis seemed to be minor when using machined surfaces. Implant surface modifications have greatly improved the first phases of osseointegration, leading to enhanced early implant success, especially in soft bone and the posterior maxilla.<sup>28</sup> However, the advantages brought by material technology in terms of osseointegration are likely to lead to a more challenging mucosal seal, especially once a lesion is established.<sup>6</sup> To facilitate an epithelial seal and reduce the chances of bacterial infiltration around the prosthesis, more basic science and clinical studies focused on epithelial cell adhesion around dental implants are needed. The present authors propose the combined method developed as an easy and rapid way to quantify cell adhesion and growth on three-dimensional scaffolds such as dental implants. This method allows precise and reliable monitoring of cell vitality, proliferation, and spreading over time. Improvement will be attained by analyzing several variables on different supports of identical size and shape (eg, different implant materials, surface topographies, and/or cell types). This new strategy combines biochemical and image-

based analyses and could be easily applied in the screening of new materials for clinical purposes and to evaluate the behavior of cells derived from donors suffering from different oral pathologies.

## Conclusions

Given the importance of peri-implant mucosal sealing in providing protection to the underlying tissues and stability to the prosthesis, this study investigated cell response to different implant surfaces. Taken together, the data support the hypothesis that the process of prosthesis sealing may be affected by the physical and topographical features of the implant, indicating that machined surfaces exert a positive influence on the proliferation rate of primary human gingival keratinocytes and gingival and epithelial progenitor cells. The results confirm that implant surface modifications have a relevant effect on epithelial cell adhesion and proliferation. Furthermore, the authors believe that appropriately designed *in vitro* experiments may be a useful and predictive tool to provide indications about implant success or failure. It seems incredibly important for implant manufacturers and researchers to evaluate the impact of different implant surfaces and designs on the establishment of a stable mucosal seal around the prosthesis. After osseointegration and connective tissue integration, the onset of a proper epithelial seal may further improve implant success.

## Acknowledgments

This study was supported by iRES Group (Lugano, Switzerland), Ministero della Salute (Ricerca Corrente: RC L2033), and the Department of Biomedical, Surgical and Dental Sciences at the University of Milan (grant no. 15-63017000-700). The authors would like to thank Dr P. Maroni and Dr A. Milani for their precious help.

## References

1. Moraschini V, Poubel LA, Ferreira VF, Barboza Edos S. Evaluation of survival and success rates of dental implants reported in longitudinal studies with a follow-up period of at least 10 years: A systematic review. *Int J Oral Maxillofac Surg* 2015;44:377–388.
2. Shimono M, Ishikawa T, Enokiya Y, et al. Biological characteristics of the junctional epithelium. *J Electron Microsc* (Tokyo) 2003;52:627–639.
3. Shibata Y, Tanimoto Y. A review of improved fixation methods for dental implants. Part I: Surface optimization for rapid osseointegration. *J Prosthodont Res* 2015;59:20–33.
4. Ellingsen JE, Thomsen P, Lyngstadaas SP. Advances in dental implant materials and tissue regeneration. *Periodontol* 2000 2006;41:136–156.
5. Atsuta I, Ayukawa Y, Kondo R, et al. Soft tissue sealing around dental implants based on histological interpretation. *J Prosthodont Res* 2016;60:3–11.
6. Derks J, Schaller D, Håkansson J, Wennström JL, Tomasi C, Berglundh T. Peri-implantitis: Onset and pattern of progression. *J Clin Periodontol* 2016;43:383–388.
7. Zitzmann NU, Berglundh T, Marinello CP, Lindhe J. Experimental peri-implant mucositis in man. *J Clin Periodontol* 2001;28:517–523.
8. Seymour GJ, Powell RN, Aitken JF. Experimental gingivitis in humans. A clinical and histologic investigation. *J Periodontol* 1983;54:522–528.
9. Berglundh T, Gislason O, Lekholm U, Sennerby L, Lindhe J. Histopathological observations of human periimplantitis lesions. *J Clin Periodontol* 2004;31:341–347.



10. Baharloo B, Textor M, Brunette DM. Substratum roughness alters the growth, area, and focal adhesions of epithelial cells, and their proximity to titanium surfaces. *J Biomed Mater Res A* 2005;74: 12–22.
11. Lin HY, Liu Y, Wismeijer D, Crielaard W, Deng DM. Effects of oral implant surface roughness on bacterial biofilm formation and treatment efficacy. *Int J Oral Maxillofac Implants* 2013;28:1226–1231.
12. Dhir S, Mahesh L, Kurtzman GM, Vandana KL. Peri-implant and periodontal tissues: A review of differences and similarities. *Compend Contin Educ Dent* 2013; 34:e69–e75.
13. Silva E, Félix S, Rodríguez-Archilla A, Oliveira P, Martins dos Santos J. Revisiting peri-implant soft tissue: Histopathological study of the peri-implant soft tissue. *Int J Clin Exp Pathol* 2014;7: 611–618.
14. Aasen T, Izpísúa Belmonte JC. Isolation and cultivation of human keratinocytes from skin or plucked hair for the generation of induced pluripotent stem cells. *Nat Protoc* 2010;5:371–382.
15. Griffin LM, Cicchini L, Xu T, Pyeon D. Human keratinocyte cultures in the investigation of early steps of human papillomavirus infection. *Methods Mol Biol* 2014;1195:219–238.
16. Sonoyama W, Liu Y, Fang D, et al. Mesenchymal stem cell-mediated functional tooth regeneration in swine. *PLoS One* 2006;1:e79.
17. de Girolamo L, Lopa S, Arrigoni E, Sartori MF, Baruffaldi Preis FW, Brini AT. Human adipose-derived stem cells isolated from young and elderly women: Their differentiation potential and scaffold interaction during in vitro osteoblastic differentiation. *Cytotherapy* 2009;11:793–803.
18. Niada S, Ferreira LM, Arrigoni E, et al. Porcine adipose-derived stem cells from buccal fat pad and subcutaneous adipose tissue for future preclinical studies in oral surgery. *Stem Cell Res Ther* 2013;4:148.
19. Esposito M, Felice P, Barausse C, Pistilli R, Grandi G, Simion M. Immediately loaded machined versus rough surface dental implants in edentulous jaws: One-year postloading results of a pilot randomised controlled trial. *Eur J Oral Implantol* 2015;8:387–396.
20. Kang BS, Sul YT, Oh SJ, Lee HJ, Albrektsson T. XPS, AES and SEM analysis of recent dental implants. *Acta Biomater* 2009;5:2222–2229.
21. Dominici M, Le Blanc K, Mueller I, et al. Minimal criteria for defining multipotent mesenchymal stromal cells. The International Society for Cellular Therapy position statement. *Cytotherapy* 2006;8: 315–317.
22. Niada S, Giannasi C, Ferreira LM, Milani A, Arrigoni E, Brini AT. 17 $\beta$ -estradiol differentially affects osteogenic differentiation of mesenchymal stem/stromal cells from adipose tissue and bone marrow. *Differentiation* 2016;92:291–297.
23. Jeon YJ, Kim J, Cho JH, Chung HM, Chae JI. Comparative analysis of human mesenchymal stem cells derived from bone marrow, placenta, and adipose tissue as sources of cell therapy. *J Cell Biochem* 2016;117:1112–1125.
24. Thorlakson HH, Schreurs O, Schenck K, Blix IJ. Lysophosphatidic acid regulates adhesion molecules and enhances migration of human oral keratinocytes. *Eur J Oral Sci* 2016;124:164–171.
25. Atsuta I, Ayukawa Y, Furuhashi A, et al. In vivo and in vitro studies of epithelial cell behavior around titanium implants with machined and rough surfaces. *Clin Implant Dent Relat Res* 2014;16:772–781.
26. Esposito M, Ardebili Y, Worthington HV. Interventions for replacing missing teeth: Different types of dental implants. *Cochrane Database Syst Rev* 2014; (7):CD003815.
27. Simion M, Gionso L, Grossi GB, Briguglio F, Fontana F. Twelve-year retrospective follow-up of machined implants in the posterior maxilla: Radiographic and peri-implant outcome. *Clin Implant Dent Relat Res* 2015;17(suppl):e343–e351.
28. Goiato MC, dos Santos DM, Santiago JF Jr, Moreno A, Pellizzer EP. Longevity of dental implants in type IV bone: A systematic review. *Int J Oral Maxillofac Surg* 2014;43:1108–1116.